Electronic states in rare-earth 1:2:3 oxides: Photoemission and Raman studies

In-Sang Yang, A. G. Schrott, C. C. Tsuei, G. Burns, and F. H. Dacol
IBM Research Division, Thomas J. Watson Research Center, Yorktown Heights, New York 10598
(Received 16 July 1990; revised manuscript received 12 October 1990)

X-ray photoemission spectra (XPS) and Raman measurements of $Y_{1-x}Eu_xBa_2Cu_3O_7$ and $Eu_{1-x}Pr_xBa_2Cu_3O_7$ are compared to those of $Y_{1-x}Pr_xBa_2Cu_3O_7$. It is shown that, with increasing x, the binding energies of the Ba core levels of $Eu_{1-x}Pr_xBa_2Cu_3O_7$ shift towards higher values as in $Y_{1-x}Pr_xBa_2Cu_3O_7$, while those of $Y_{1-x}Eu_xBa_2Cu_3O_7$ do not, despite similar changes in Ba-O interatomic distances in the latter two systems. Raman measurements of $Y_{1-x}Pr_xBa_2Cu_3O_7$ show a frequency increase of the Ba and apical-oxygen modes with increasing x, but a much smaller frequency increase in $Y_{1-x}Eu_xBa_2Cu_3O_7$. The XPS and Raman results reflect changes in the Ba-O hybridization and correlate with both the suppression of superconductivity in both $Y_{1-x}Pr_xBa_2Cu_3O_7$ and $Eu_{1-x}Pr_xBa_2Cu_3O_7$, and with the retention of superconductivity in $Y_{1-x}Eu_xBa_2Cu_3O_7$.

In a previous paper of XPS measurements of the $Y_{1-x}Pr_xBa_2Cu_3O_7$ (Y-Pr 1:2:3) system,[1] we observed that the binding energies of the Ba core levels shifted towards higher values with increasing x, suggesting hole localization on Ba sites. We speculated that this hole localization might be associated with the suppression of superconductivity in the Y-Pr 1:2:3. Our polarized Raman measurements[2] of Y-Pr 1:2:3 support the hole-localization idea and indicate that the holes (localized at Ba sites) may come from a bonding band of Ba-O_z, where O_z is an apical-oxygen atom. However, since replacement of Y by Pr increases the interatomic distances, the XPS and Raman measurements may simply reflect such changes, rather than being related to the suppression of superconductivity in Y-Pr 1:2:3. In order to further understand the observed effects, we have examined XPS and Raman spectra of the $Y_{1-x}Eu_xBa_2Cu_3O_7$ (Y-Eu 1:2:3) and $Eu_{1-x}Pr_xBa_2Cu_3O_7$ (Eu-Pr 1:2:3) systems. The rationale for these experiments is given by the fact that superconductivity is not suppressed in Y-Eu 1:2:3 while it is strongly suppressed in Eu-Pr 1:2:3 even though changes in interatomic distances in Y-Eu 1:2:3 as Y is replaced by Eu are similar to those in Y-Pr 1:2:3. We show that the XPS energy shifts of the Ba core levels in Y-Pr 1:2:3 and Eu-Pr 1:2:3 and the frequency increases of the Ba and O_z modes in Raman of Y-Pr 1:2:3 are not just related to changes of interatomic distances but to changes in Ba-O hybridization which might be, in turn, related to superconductivity.

Details of the preparation method and characterization for Y-Eu 1:2:3 samples were discussed previously,[3] and a similar method was used for Eu-Pr 1:2:3. Powder x-ray diffraction patterns showed insignificant amounts of impurity phases, not correlated with Pr concentration. Values of T_c and 10–90 % transition-width ΔT_c of Eu-Pr 1:2:3 determined by resistance versus temperature measurements are shown in Table I, along with those of Y-Pr 1:2:3 and Y-Eu 1:2:3. Samples of $x=0.6$ or higher show semiconducting behavior and no superconductivity down to 4 K.

Photoemission measurements were done in a VG ESCALAB MK II system with a monochromatic Al $K\alpha$ source, at room temperature. The background pressure of the spectrometer was 7×10^{-10} torr. All of the measured samples were scraped *in situ* at room temperature using a tungsten knife. The Ba 3*d* and 4*d* levels along with the Cu 3*p*, Cu 2*p*, C 1*s*, O 1*s*, and other core and valence levels were measured. No charging effects were observed except in $PrBa_2Cu_3O_7$. The Raman measurements were performed at room temperature with $x(zz)\bar{x}$ and $z(xx)\bar{z}$ polarizations[4] using a focused beam in backscattering geometry on single crystals embedded in ceramic samples.

The XPS spectra of all the samples were not significantly different from each other. The scraped samples exhibited insignificant intensity in the C 1*s* region, around 289 eV, and a small shoulder in the O 1*s* region around 531 eV (see Fig. 2 in Ref. 1). This is characteristic of well-prepared polycrystalline samples with little carbonate contamination.[5] Small variations from sample to sample in the intensity of the feature at 531 eV did not correlate with Pr concentration. The valence spectra exhibited significant intensity at the Fermi energy for $x\leq0.4$. Figure 1(a) shows the valence spectrum for $Eu_{0.8}Pr_{0.2}Ba_2Cu_3O_7$. This spectrum is very similar to that of single crystal Y 1:2:3 cleaved in vacuum and shown in Fig. 1(b) (reproduced from Fig. 2 in Ref. 6), in particular, in the region near the Fermi energy. As for the Ba 5*p* region, our spectrum resembles more the dashed curve in Fig. 1(b), which is described as arising from regions of the surface having higher cleavage damage. A second component (aside from that due to carbonate[5]) at $\simeq1$ eV higher binding energy, has been often described in the Ba core levels of 1:2:3 oxides.[6–8] This second feature has been related to a local chemical environment for Ba at the surface different from that of bulk Y 1:2:3,[6–8] and the difference in binding energy has been explained either by final-state effects, namely, a decrease

TABLE I. T_c determined by the midpoint of the resistivity drop, and 10–90 % transition widths, ΔT_c (in parentheses), as a function of x.

x	Y-Pr 1:2:3	Eu-Pr 1:2:3	Y-Eu 1:2:3
0.0	91.5 (1.5)	94.1 (0.9)	92.2 (0.9)
0.2	71.4 (3.2)	61.4 (2.3)	
0.4	41.3 (6.2)	19.8 (8.5)	92.9 (1.0)
0.6			
0.8			94.1 (1.1)
1.0			95.1 (0.6)

in screening resulting from a lower oxygen coordination,[9] or more recently by electrostatic effects arising from different lattice parameters associated with the tetragonal phase.[10] This surface phase, which is also likely to be produced by scraping damage, is less evident in the XPS regime than in spectra taken with the synchrotron source, because of the much lower photoelectron kinetic energy typically involved in the latter. Therefore, although the surface effects have to be considered in analyzing our spectra, they are not expected to totally interfere with the signal more representative of the bulk.

The Cu $2p$ spectra of Y-Eu 1:2:3 showed no change with x, while those of Eu-Pr 1:2:3 showed changes in the intensity ratio of main-to-satellite peaks. These changes were produced mainly by the overlap with the Pr $3d$ peaks, and masked any intrinsic variation of the Cu spectra. In Y-Eu 1:2:3, there was no change in all the observed core levels with x. In Eu-Pr 1:2:3, however, the binding energies of the Ba $3d$ and $4d$ peaks increased with Pr doping. The binding-energy shifts Δ defined in Fig. 2(a), are shown as a function of x in Fig. 2(b) for Y-Pr 1:2:3, Y-Eu 1:2:3, and Eu-Pr 1:2:3. Note that the x dependence of the binding-energy shifts of the Ba $3d$ and $4d$ peaks of Eu-Pr 1:2:3 are essentially the same as those in Y-Pr 1:2:3. On the other hand, no energy shift was observed for Y-Eu 1:2:3. In Fig. 3, the phonon frequencies of the Ba and O_z modes versus x are shown for Y-Eu 1:2:3 and Y-Pr 1:2:3. The frequency increases of the two modes in Y-Eu 1:2:3 are much smaller than those in Y-Pr 1:2:3 despite similar increases in interatomic distances in both systems.[11,12] In fact, due to a bond-length increase, we normally would expect a decrease in the phonon frequencies.

It is conceivable that the growth of a second spin-split component in our spectra may produce an effective

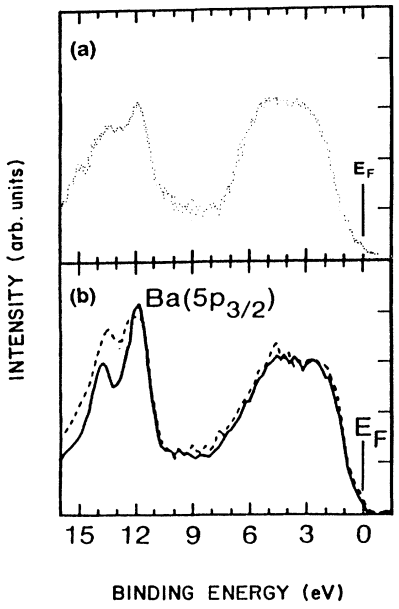

FIG. 1. XPS valence spectra. (a) $Eu_{0.8}Pr_{0.2}Ba_2Cu_3O_7$, polycrystalline sample, scraped *in situ*. (b) $YBa_2Cu_3O_7$, single crystal cleaved *in situ* (from Ref. 6).

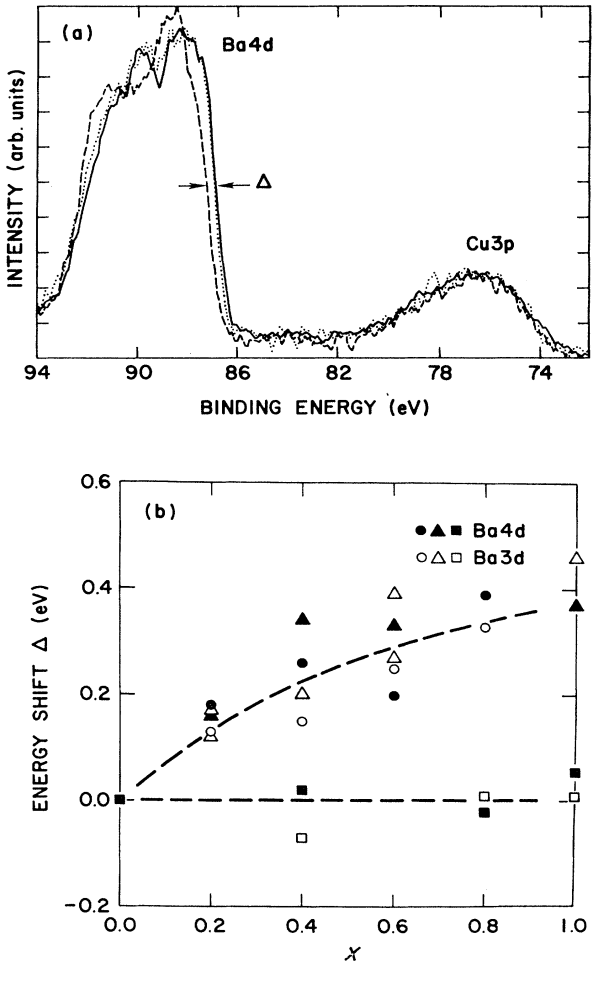

FIG. 2. (a) Ba $4d$ and Cu $3p$ XPS peaks for $YBa_2Cu_3O_7$, solid curve; $EuBa_2Cu_3O_7$, dotted curve; and $Eu_{0.4}Pr_{0.6}Ba_2Cu_3O_7$, dashed curve. The binding-energy shift Δ is defined as noted. (b) Plot of the binding-energy shift Δ, vs x for $Y_{1-x}Pr_xBa_2Cu_3O_7$ (circles), $Eu_{1-x}Pr_xBa_2Cu_3O_7$ (triangles), and $Y_{1-x}Eu_xBa_2Cu_3O_7$ (squares).

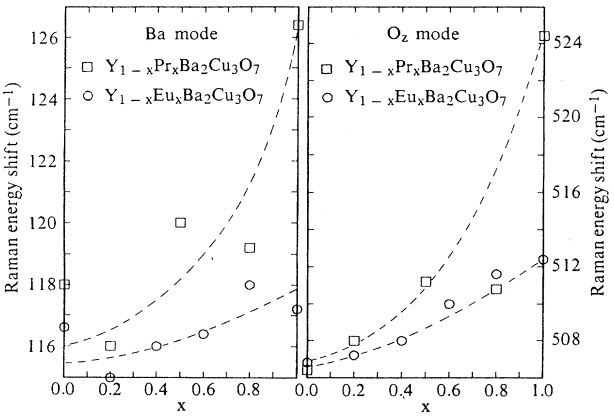

FIG. 3. The Raman frequency increase of Ba and O_z modes vs x for $Y_{1-x}Pr_xBa_2Cu_3O_7$ and $Y_{1-x}Eu_xBa_2Cu_3O_7$.

binding-energy shift such as that shown in Fig. 2. Due to the peak broadening inherent to the scraping process, our XPS spectra do not have the resolution required to directly discern whether the shift is a real one. Therefore we have tried to deconvolute the curves in Fig. 2(a) using three spin-split components corresponding to the bulk 1:2:3 phase (1), a surface phase due to damage (2), and a contaminant phase (3), respectively. Figure 4(a) shows the best fit to the Ba 4*d* for Eu 1:2:3 of Fig. 2(a). The positions of peaks 1 and 2 agree with those assigned to the bulk and surface components (see Ref. 6, and references therein). The position of peak 3 corresponds to that of Ba 4*d* in $BaCO_3$, and its relative intensity is consistent with that of the feature at 531 eV in the O 1*s* spectra.[1] Figure 4(b), solid curve, shows the best fit to Ba 4*d* in $Eu_{0.6}Pr_{0.4}Ba_2Cu_3O_7$ [dashed curve in Fig. 2(a)]. Shifts of 0.4 eV in component 1, and of 0.2 eV in component 2 were necessary to fit the data. The shift in component 2 is justified considering that this component probably arises from surface damage and therefore may not be totally independent from the bulk one. The small increase in component 3 (not shifted) is consistent with the variations found in the O 1*s* feature at 531 eV. Figure 4(c), represents the best fit to the same data as in Fig. 4(b), with the original components restricted to changes in intensity only. In this case, we did not obtain a very good fit (solid curve) to the data. If component 2 is increased with respect to 1, the minimum around 90.2 eV becomes more pronounced. If the opposite is tried, the leading edge moves out of range. An increase in component 3 produces a shoulder not found in the data. Thus, the results of Fig. 4 indicate a real shift in the bulk component of the Ba 4*d* XPS peak, and are consistent with the x-ray data and more importantly with the Raman spectra which clearly showed a continuous shift with x. These spectra are easier to discern since the width of the Raman peaks are narrower than the observed frequency change (see Fig. 2 in Ref. 2). Similar continuous shifts have also been observed in Y 1:2:3 as a function of oxygen content.[1,13] Therefore, we conclude that the Ba core levels exhibit a real shift with Pr concentration. This shift is not produced by a different oxygen concentration,[1] which do not decrease in Pr-doped 1:2:3 samples. Moreover, the shifts of the Ba core levels do not correlate with

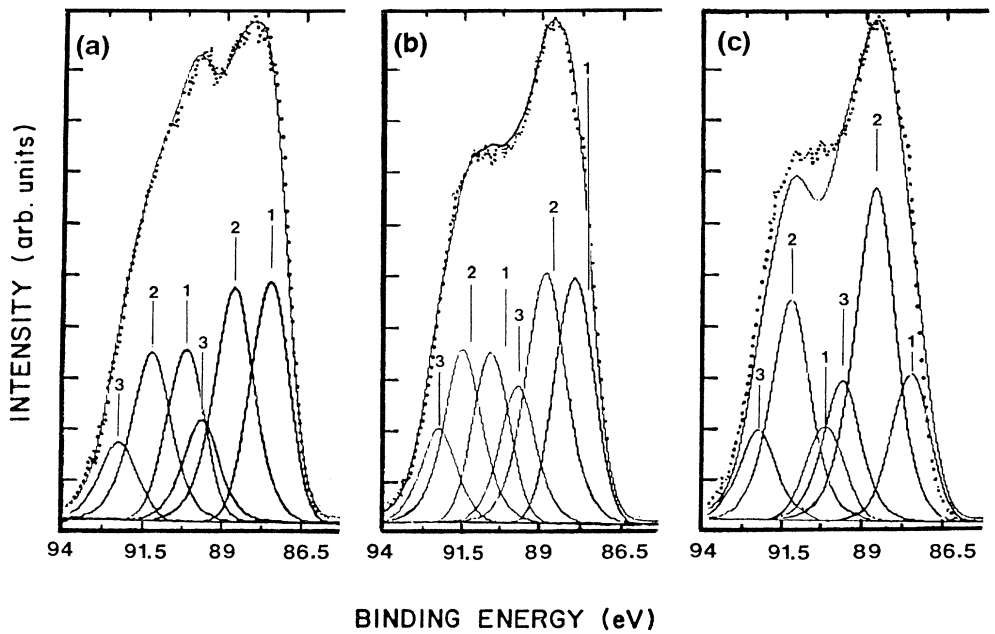

FIG. 4. Best fit to the curves in Fig. 2(a). The components are described in the text, the peak synthesis is shown in solid lines. (a) $EuBa_2Cu_3O_7$ (dots). (b) $Eu_{0.4}Pr_{0.6}Ba_2Cu_3O_7$ (dots), with shifts in components 1 and 2. (c) $Eu_{0.4}Pr_{0.6}Ba_2Cu_3O_7$ (dots), with no shift in the components.

changes in interatomic distances but do correlate with suppression of superconductivity in the Pr-doped systems. Thus, we believe that these shifts reflect changes in the Ba-O overlap in the initial state. This is supported by the Raman results which will be discussed below. Wertheim[14] has suggested that while the 5*d* band in metallic Ba is almost empty, Ba 5*d* states play a significant role in the bonding of Ba compounds. A partial occupation of 5*d* orbitals, with smaller radial extent than the 6*s* ones, may have a strong effect in decreasing the observed binding energies. According to this, the binding-energy increase of the Ba core levels with increasing x in Y-Pr 1:2:3 and Eu-Pr 1:2:3 indicates more localized holes with Ba 5*d* character as the Pr doping increases in both systems. Accordingly, no such hole localization in Y-Eu 1:2:3 occurs as Eu doping increases. The larger frequency increases of the Ba and O_z Raman modes in Y-Pr 1:2:3 implies that the Ba-O overlap integral gets larger for larger Pr doping. Therefore, we conjecture that changes in Ba-O overlap result in charge transfer from a Ba-O molecular band which has strong Ba 5*d* character to a Ba-O bonding band such as Ba 6*s*–O 2*p*, as Pr doping increases. This will result in a higher degree of hole localization at Ba 5*d* sites in Pr 1:2:3 than in Y 1:2:3 (and in Eu 1:2:3). These changes are schematized in Fig. 5.

It has been suggested that the Ba-O planes may play a role as electron charge reservoirs,[15,16] which control the charge states of the CuO_2 planes. Our XPS and Raman results seem to underscore the importance of the interplay between Ba-O planes and CuO_2 planes in attaining high-temperature superconductivity in 1:2:3 structures. Furthermore, they are fingerprints of good superconductors behavior in 1:2:3. In this context, we expect that the binding energies of the Ba core levels even in $LaBa_2Cu_3O_7$, which has largest lattice constants among rare-earth 1:2:3, should be the same as those in $YBa_2Cu_3O_7$.

In summary, we have observed XPS and Raman spectra of $Y_{1-x}Eu_xBa_2Cu_3O_7$ and $Eu_{1-x}Pr_xBa_2Cu_3O_7$, and compared the results with those of $Y_{1-x}Pr_xBa_2Cu_3O_7$. In contrast to Y-Pr 1:2:3, no Ba core-level shift in Y-Eu 1:2:3 was detected throughout the entire range of x, despite similar changes in lattice parameters in both systems. On the other hand, in Eu-Pr 1:2:3 we found similar Ba core-level shifts to those found in Y-Pr 1:2:3, despite smaller lattice-parameter changes in Eu-Pr 1:2:3 than in Y-Pr 1:2:3. Therefore, we conclude that this Ba core level shifts in Y-Pr 1:2:3 and Eu-Pr 1:2:3 do not directly arise from changes in interatomic distances, as it has been recently proposed for the tetragonal phase of the oxygen deficient Y 1:2:3,[11] but from changes in the Ba-O covalency. From Raman measurements, we inferred that XPS shifts reflect changes in the initial state. Both XPS and Raman results are consistent with changes in Ba-O hybridization reflecting charge transfer from a Ba-O band of Ba 5*d* character to a Ba-O band of Ba 6*s* character in Pr-doped 1:2:3, which may lead to an effective hole localization at Ba sites. This hole localization is related to the suppression of superconductivity in Y-Pr 1:2:3 and Eu-Pr 1:2:3.

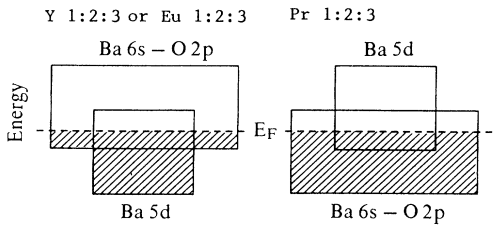

FIG. 5. A schematic drawing of relative energy levels of the Ba 6*s*–O 2*p* bonding band and a Ba-O band which has dominant Ba 5*d* character (denoted as Ba 5*d*). Since the Ba 5*d* band is more localized than Ba 6*s*–O 2*p* band, it is drawn narrower than Ba 6*s*–O 2*p*.

The authors wish to thank J. F. Bringley and J. P. Berosh for some of the samples.

[1]In-Sang Yang, A. G. Schrott, and C. C. Tsuei, Phys. Rev. B **41**, 8921 (1990).

[2]In-Sang Yang, G. Burns, F. H. Dacol, and C. C. Tsuei, Phys. Rev. B **42**, 4240 (1990).

[3]In-Sang Yang, G. Burns, F. H. Dacol, J. F. Bringley, and S. S. Trail, Physica C **171**, 31 (1990).

[4]G. Burns, F. H. Dacol, P. Freitas, T. Plaskett, and W. König, Solid State Commun. **64**, 471 (1987); G. Burns, F. H. Dacol, F. Holtzberg, and D. L. Kaiser, *ibid.* **66**, 217 (1988).

[5]A. G. Schrott, S. L. Cohen, T. R. Dinger, F. J. Himpsel, J. A. Yarmoff, K. G. Frase, S. I. Park, and R. Purtell, in *Thin Film Processing and Characterization of High-Temperature Superconductors,* edited by J. M. E. Harper, R. J. Colton, and L. C. Feldman, AIP Conf. Proc. No. 165 (AIP, New York, 1987), p. 349.

[6]D. E. Fowler, C. R. Brundle, J. Lerczak, and F. Holtzberg, J. Electron Spectrosc. Relat. Phenom. **52**, 323 (1990).

[7]P. Steiner, V. Kisinger, I. Sander, B. Siegwart, S. Hüfner, and C. Politis, Z. Phys. B **67**, 19 (1987).

[8]R. Liu, C. G. Olson, A.-B. Yang, C. Gu, D. W. Lynch, A. J. Arko, R. S. List, R. J. Bartlett, B. W. Veal, J. Z. Liu, A. P. Paulikas, and K. Vandervoort, Phys. Rev. B **40**, 2650 (1989).

[9]R. S. List, A. J. Arko, Z. Fisk, S.-W. Cheong, S. D. Conradson, J. D. Thompson, C. B. Pierce, D. E. Peterson, R. J. Bartlett, N. D. Shinn, J. E. Schirber, B. W. Veal, A. P. Paulikas, and J. C. Campuzano, Phys. Rev. B **38**, 11966 (1988).

[10]F. Parmigiani, G. Pacchioni, C. R. Brundle, D. E. Fowler, and P. S. Bagus, Phys. Rev. B **43**, 3695 (1991).

[11]G. Burns and A. M. Glazer, in *Space Groups for Solid State Scientists* (Academic, San Diego, 1990), Chap. 9.

[12]R. M. Hazen, in *Physical Properties of High Temperature Superconductors II,* edited by D. M. Ginsberg (World Scientific, Singapore, 1990), and papers cited therein.

[13]R. Feile, Physica C **159**, 1 (1989).

[14]G. K. Wertheim, J. Electron Spectrosc. Relat. Phenom. **34**, 309 (1984).

[15]K. A. Müller, Z. Phys. B **80**, 193 (1990).

[16]R. J. Cava, Science **247**, 656 (1990).